NUMERICAL INVESTIGATIONS ON THE EFFECT OF HUMIDITY AND WATER INGESTION ON THE PERFORMANCE OF A SUBSONIC AXIAL FLOW COMPRESSOR

Aaron SEQUEIRA[1], Pramod SALUNKHE*[2], Mahesh VARPE[3]

This study investigates the influence of relative humidity and ingestion of water in an aerosol form on the aerodynamic performance of a subsonic axial flow compressor. The numerical simulations were carried out using ANSYS© CFX solver. The humidified air had detrimental effect on the compressor performance resulting in increase in relative humidity, reduction in static pressure rise by 8% and 5% decrease in the maximum isentropic efficiency. On the contrary, the ingestion of micro-water droplets into the compressor enhanced the efficiency with a reduction in specific work input. This was attributed to evaporative cooling induced by the water droplets.

Keywords: water ingestion, stability of axial flow compressor, compressor performance

1. Introduction

Axial compressors are widely used in the aerospace and industrial sectors owing to their ease of incorporation into larger systems and ability to perform consistently better under varying ambient conditions. They also boast higher efficiencies and pressure ratios when compared to their centrifugal or radial counterparts. The effect of moisture on the performance and operating limits of an axial compressor is an extensively researched topic, however, the mechanism of aero-hydrodynamics is still not clear or understood completely. Moisture may exist naturally in the air as humidity or be introduced artificially through the use of sprays. Wet compression is an established concept that allows for efficient compression. Many novel compressor designs incorporate mechanisms for water injection, in an attempt to utilize the wet compression cycle. Thus, it is of interest

[1]Student, Dept. of Aeronautical & Automobile Engg. Manipal Institute of Technology, Manipal Academy of Higher Education, Manipal, India, e-mail: aaronduanes@gmail.com
[2]*Assoc. Prof., Dept. of Aeronautical & Automobile Engg. Manipal Institute of Technology, Manipal Academy of Higher Education, Manipal, India, e-mail: pramod.salunkhe@manipal.edu (corresponding author)
[3]Assoc. Prof., Dept. of Aerospace Engg., M. S. Ramaiah University of Applied Sciences, Bengaluru, Karnataka, India, e-mail: maheshkvarpe.aae.et@msruas.ac.in

to further comprehend the mechanism of wet compression in improved aerodynamic performance.

Berdanier et al. [1] devised a novel method to accurately predict the compressor performance by taking into account the effect of humidity of the incoming air, assuming it as a real gas. A multi-stage compressor was used to gather experimental data for various absolute humidity levels. The study also provided an analytical treatment of humidity, its effect on the compressor performance and the parameter correction process. It was reported that the varying humidity caused moderate effects on the compressor performance. Rhee et al. [2] experimentally and numerically investigated the effect of varying relative humidity on a compressor cascade at Mach 1.11. The experimental data was obtained through the use of a transonic wind-tunnel. Numerical simulations were carried out through the incorporation of classical nucleation theory and the Hertz-Knudsen droplet growth model into a CFD solver. It was observed that increasing the humidity level resulted in reduction in total pressure and loss coefficient through the heat addition and condensation.

Tomita et al. [3] investigated the effects of humid air with water injection on the performance of an axial flow compressor in transonic flow regime. The streamline curvature program was used as a numerical tool for the calculation of various compressor performance parameters. The program was modified to allow for humidity variation and the injection of water droplets. The influence of absolute humidity, particle diameter and injection rate on flow properties such as pressure, temperature and density were studied at different axial locations. It was reported that the humidity reduced the compressor performance, whereas, the injection of water droplets resulted in increased isentropic efficiency. Subsequently, White and Meacock [4] examined the impact of the evaporative effects of water injection on compressor operation, assuming that evaporation occurs primarily within the compressor itself, and not in the inlet. The thermodynamic equations for fluid compression were augmented through the introduction of an expression for droplet evaporation. Numerical methods were employed to solve the system of equations to determine the compressor off-design performance. A strong dependence on droplet diameter was noted, as well as a narrowed efficiency peak. The calculations also revealed that water injection shifted the compressor characteristics to higher mass flows and pressure ratios.

There exists abundant literature on the effects of humidity and water injection on the compressor performance which is limited to high speed axial flow compressor. Further studies related to the effects of varying humidity on the compressor performance coupled with the ingestion of an aerosol form of water, is also quite rare. This motivated to pursue the investigations as reported in the present work.

2. Computational domain

The reference compressor geometry selected is a low-speed subsonic axial flow compressor manufactured by the Royston Fan Corporation. This compressor has been used in a number of studies by Roos [5], Gill [6] and Hamman [7]. Table 1 lists the basic compressor design parameters. The blade profile used for the reference compressor is modified NACA-65 series airfoil. The blades in both the rotor and stator have chord of 30 mm, span of 60 mm and a profile thickness of 10% of the chord, with the airfoil camber varying from hub to tip. The rotor row within each stage consists of 43 blades while the stator row consists of 41 blades with a rotor-stator inter-stage spacing of 22 mm. Figure 1 depicts the computational domain for the present work.

Table 1

Compressor Design Parameters

Parameter	Value
No. of Stages	3 Repeating
Design Speed	3000 RPM
Design Flow rate	2.7 kg/s
Reaction	0.82
Hub Radius	150 mm
Hub-to-Tip Ratio	0.71
Blade Aspect Ratio	2

For the present simulations, only a single compressor stage was modelled and computationally simulated. The complete three-stage performance curve was extrapolated from the results of a single stage using analytical approximations. Additionally, the domain encompassed only a single blade row, as opposed to the full annulus. This was done to further refine the solution process, with flow through the neighbouring blade passages simulated by the use of rotational periodicity. The effects of tip clearance were neglected for the sake of simplicity. This has greatly reduced the computational time and resources.

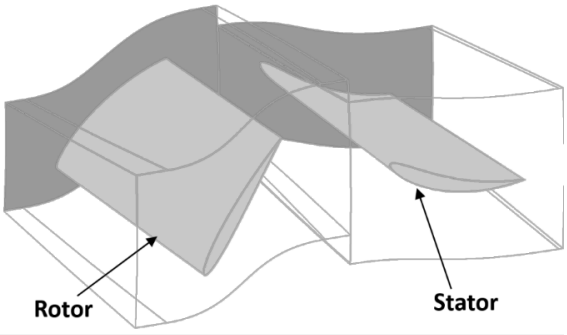

Fig. 1. An isometric view of the computational domain

3. Mesh generation

The computational domain was discretized using the ANSYS TurboGrid meshing module using its Automated Topology and Mesh (ATM) technology, as shown in Fig. 2. Elements were generated around the blades using an O-Grid mesh while H-Grid was employed for the inlet and outlet passages. A global size factor (GSF) was used to control the mesh size within a blade and inlet and outlet passages. Refinement within the boundary layer was adjusted to conform to the desired value of the non-dimensional wall sizing parameter y^+. Table 2 lists the average and maximum values of y^+ obtained for different wall regions within the domain. The global average was found to lie in the range of 1 - 2, indicating that the laminar sub-layer was resolved to a sufficient degree.

Table 3 shows the number of elements for each mesh refinement level and the calculated pressure ratio. It was observed that the change in pressure ratio from the Level 2 to Level 3 was of the order of 0.001% and was hence considered negligible. Thus, all the simulations were carried out with a Level 2 mesh consisting of 0.613 million elements, in lieu of the computational costs associated with the higher levels of refinement.

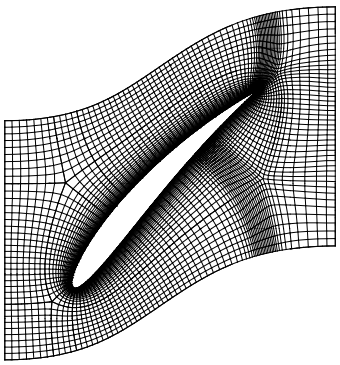

Fig. 2. A mid-span section of the structured, hexahedral mesh generated using ATM for the rotor blade passage

Additionally, the quality, viz., the aspect ratio and orthogonality, of the computational grid was deemed satisfactory to analyze the phenomenon. The RMS residual convergence criterion was set to a tolerance of 10^{-5}. The particle source change rate tolerance was chosen to be 10^{-2}, as recommended by the CFX Solver Modelling Guide [8].

Table 2

y^+ values of different wall regions in the domain

Location	Rotor		Stator	
	Avg.	Max	Avg.	Max
Blade	2.53	6.76	1.52	4.05
Hub	2.37	5.79	1.37	4.28
Shroud	2.89	6.67	1.32	3.71

Table 3

Mesh refinement

Refinement	No. of Elements	Pressure Ratio	Variation (%)
Level 1	325,454	1.01133	--
Level 2	613,339	1.01154	0.021
Level 3	958,677	1.01155	0.001

4. Boundary conditions and turbulence

The total pressure and mass flow were selected as the inlet and outlet boundaries, respectively. The inlet total pressure was set as 1 atm, whereas, total temperature was kept as 298 K. The mass flow rate was varied from 2.3 - 3.3 kg/s to compute the off-design performance. The density and axial velocity at the compressor inlet were derived from the specified boundary conditions by the solver. The computational domain was divided into rotating and stationary sub-domains, incorporating the Multiple Reference Frame (MRF) technique to model flow through the compressor as a steady state problem. A mixing-plane model was used at the interface between the two sub-domains, while the pitch-wise boundaries were set to be rotationally periodic. The blades, hub and shroud were set to be stationary, no-slip walls, relative to their local frame of reference.

The k-ω Shear Stress Transport (SST) model developed by Menter [9] was used to simulate turbulence in the flow, along with an automatic wall function feature in CFX that transitioned between a low Re model and a wall function model based on the local y^+ value within the boundary layer mesh.

5. Humidity model

Relative humidity (RH) is the metric used to study the effect of moisture on compressor performance, with the saturation pressure of water vapour at a particular temperature derived from the empirical August-Roche-Magnus equation [10]. The mass fraction distribution of water vapour within the compressor was considered through the use of a transport equation, taking into account advection as well as diffusion of the species. The mass fraction of air was calculated from a simple constraint equation. The transport and constraint equations solved by CFX are provided below:

$$\frac{\partial}{\partial t}\left(\rho Y_{H_2O}\right) + \nabla.\left(\rho \vec{V} Y_{H_2O}\right) = -\nabla.\vec{J}_{H_2O} \tag{1}$$

$$\sum_{i=A,B}^{N_C} Y_i = 1 \tag{2}$$

The inlet boundary mass fraction of water vapour was calculated from the relative humidity. The performance of the compressor was analysed at RH levels

of 0 (dry state), 30, 50, 70 and 90% by varying the mass fraction of water vapour at the boundary.

6. Water ingestion model

Numerical modelling of water ingestion was approached using a coupled Eulerian-Lagrangian multi-phase formulation. Here, the liquid phase is assumed to exist as a distribution of discrete particles whose movement through the domain is tracked in the Lagrangian frame of reference [10]. To model the ingestion of a fog-like aerosol, the liquid water content (LWC) and average droplet diameter were used to calculate solver inputs such as the number of droplets injected at the inlet boundary and the total droplet mass flow rate. Various studies conducted to determine the size distributions of water droplets in fog were carried out by Zak [11] and Podzimek [12]. Based on the available data, the numerical solution was run at a LWC of 0.1 g/m^3 and uniform droplet diameter distributions of 10 μm, 30 μm and 50 μm.

Aerodynamic forces on the droplets and the heat transfer were determined using the Schiller-Naumann and Ranz-Marshall particle models [13], respectively. The droplet-wall interaction was set to be an elastic collision, to simplify the physics of the model. The mass transfer due to droplet evaporation was accounted by the introduction of source terms into the continuity equation of the gas phase. In addition to varying droplet diameter, aerosol ingestion was simulated at varying relative humidity of 10 and 90% with an inlet particle temperature of 298 K.

7. Validation

The present numerical simulations were validated with the available experimental data [6,7] in terms of compressor performance map as shown in Fig. 3. The single stage results were extrapolated to approximate the full three stage performance using the following equation [7, 14] for the reference compressor.

$$\Delta p_{17} = 2.891 \Delta p_{13} \tag{3}$$

The two curves in Fig. 3 show reasonable agreement close to the compressor design point with a maximum deviation of approximately 7.5% near the stall point. Due to the limitations of the mixing plane model, the numerical estimations of compressor performance around the stall point were not in satisfactory agreement with the experimental data, hence, they were not considered for this study.

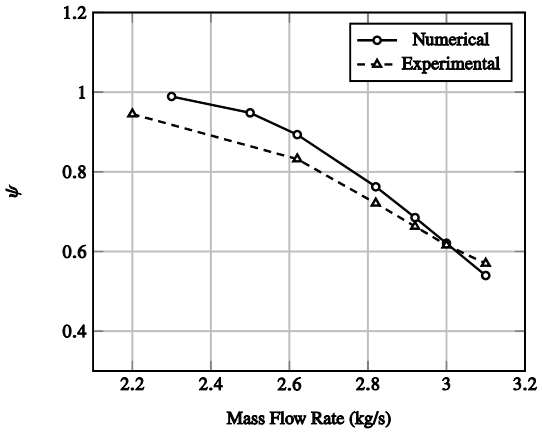

Fig. 3. Validation of present numerical results

8. Results and discussion

8.1 Effect of humidified airflow

Figure 4 depicts the local relative humidity variation in the compressor stage for the ambient relative humidity level of 50%. RH is directly proportional to the concentration of water vapour and inversely proportional to the density. It was observed that the local RH is highest at the leading edge of the rotor and reduces towards the stator trailing edge. Also, it was found that the local RH is high on the blade suction surface as compared to the pressure surface. This is attributed to the increase in flow velocity and drop in local static pressure.

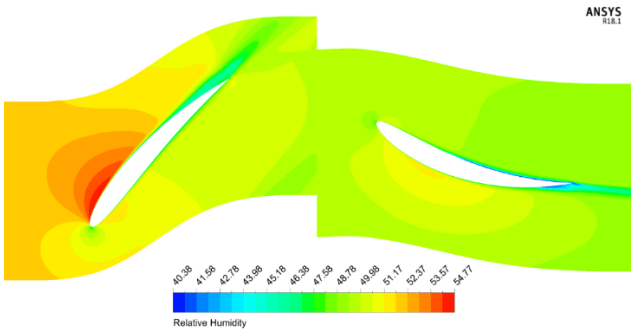

Fig. 4. Local RH variation at an ambient RH of 50%, at the mean-line radius and design flow rate.

Figure 5 shows the effect of relative humidity on the pressure rise coefficient. With reduction in relative humidity the pressure rise was found to be proportional. The highest pressure rise was obtained at the 0% RH. Subsequently, the compressor characteristics were plotted for the 0 (i.e. dry air), 30, 50, 70 and 90% relative humidity levels as shown in Fig. 6. The dry air resulted in the best compressor performance. It was observed that with increase in relative humidity, the

compressor performance deteriorates. The lowest performance was observed with 90% relative humidity with a pressure loss of around 8%.

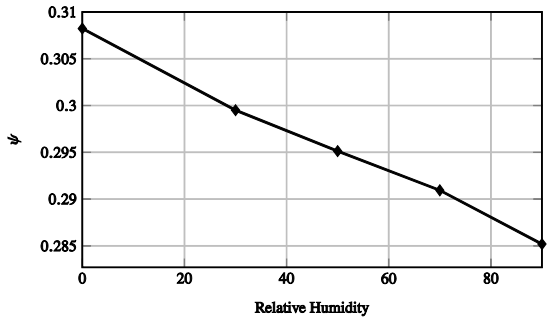

Fig. 5. Variation of the pressure rise coefficient (ψ) with relative humidity, at the design mass flow rate.

The above results appear to be in agreement with the analytical predictions of Berdanier [1] for a compressor operating with humidified airflow. As the stall point is approached, flow begins to separate over the rotor blades. This separated flow affects the diffusion of water vapour in the air and modifies the dependency of the pressure rise coefficient on the RH level.

Figure 7 shows variation in isentropic compressor efficiency with the flow coefficient for various relative humidity levels. For a given relative humidity, with reduction in flow coefficient the efficiency was found to increase, attains the peak value and later reduces.

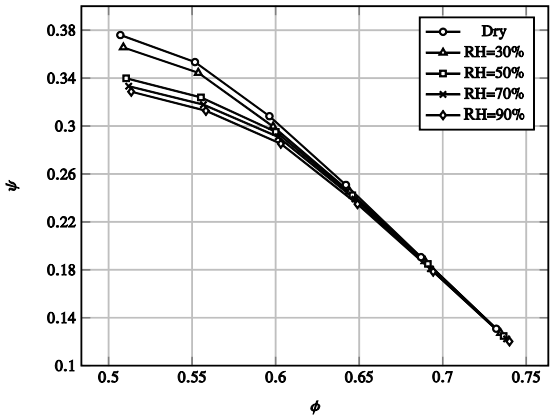

Fig. 6. Variation of static pressure coefficient (ψ) with the flow coefficient (ϕ)

With increase in relative humidity the compressor efficiency was observed to reduce and is attributed to the change in thermodynamic properties of the gas due to the presence of water vapour. This implies that for the given pressure ratio, the compressor work input increases with increase in relative humidity. The maximum reduction in isentropic compression efficiency was about 5% corresponding to RH

of 90%. It was also observed that the relative humidity has mild effect on the stall margin. The stall margin was found to improve marginally by 1% with the relative humidity of 90%.

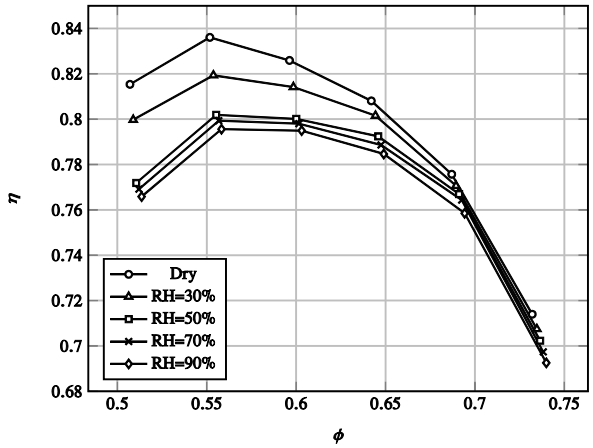

Fig. 7. Variation of isentropic efficiency (η) with the flow coefficient (ϕ)

8.2 Effect of water ingestion

The results of the water ingestion simulations show similarity to those established by wet compression theory. The ingested water droplets evaporate as they move through the compressor flow passage, absorbing energy from the fluid in its vicinity. This leads to evaporative cooling, lowering the temperature of the bulk fluid, and hence reducing the required compression work input [4]. Figure 8 shows the average path history of the ingested droplets. The coupling between the primary flow and the droplets leads to their pathways through the compressor being heavily influenced by the local flow velocity. This affects the distribution of the droplets within the domain which influences the local relative humidity, changing the local flow velocities. The two-way interaction eventually reaches a state of equilibrium. As these droplets were assumed to collide elastically with the wall boundaries, the effects of the formation of wall films were neglected.

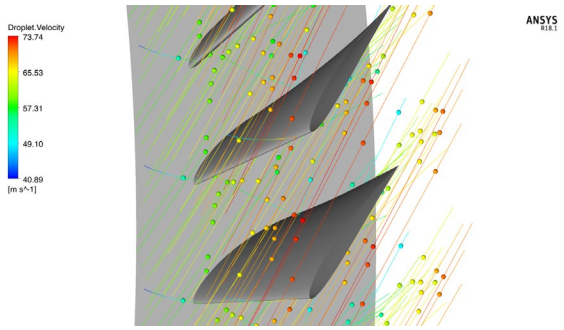

Fig. 8. Particle tracks through the rotor

Figure 9 shows the effect of droplet size on the compressor characteristics for a relative humidity of 10%. It was observed that the humidified air moderately shifted the compressor characteristics, however, the effect of droplet diameter was found to be negligible on the compressor characteristics.

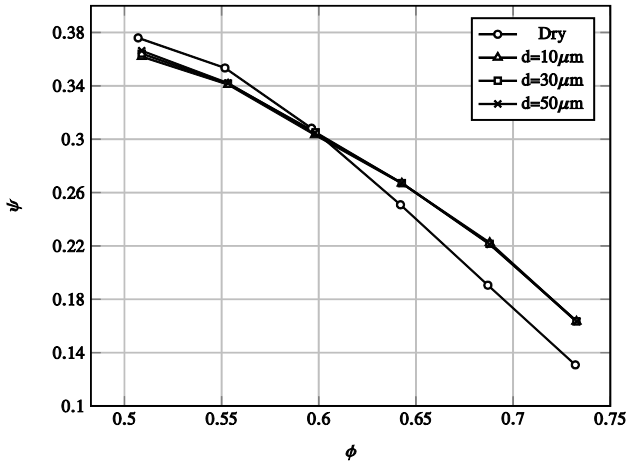

Fig. 9. Variation of the static pressure coefficient (ψ) with the flow coefficient (ϕ) at a relative humidity of 10%

This shows that the droplet diameter does not play an important role in the compressor performance. Interestingly, at higher flow coefficient the pressure rise was more for water ingestion, however, with reduction in flow coefficient it reduced as compared to that of dry air. The shift in the pressure rise curve in the presence of water ingestion was also observed by Yang et al. [15], albeit to a much lesser degree.

Figure 10 represents the variation of isentropic efficiency of the compressor for the relative humidity of 10 and 90%. The evaporative cooling effect induced by the water droplets lowers the stage outlet total temperature and hence reduces the compressor work input and increases the isentropic efficiency. The dependence of isentropic efficiency on the droplet diameter was found to reduce with increase in relative humidity from 10 to 90%. A relative humidity of 10%, the compressor exhibited higher isentropic efficiency, however, with increase in relative humidity to 90%, the isentropic efficiency was reduced by about 2.5%.

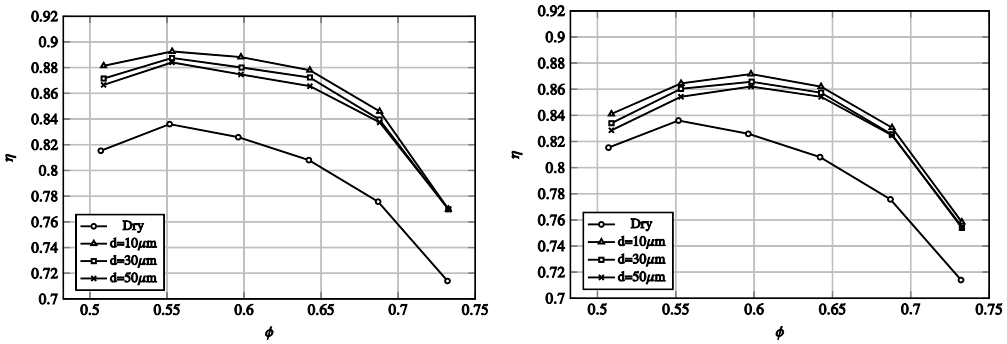

Fig. 10. Variation of isentropic efficiency with the flow coefficient at a relative humidity of (a) 10% and (b) 90%

It was also observed that the flow coefficient at the peak isentropic efficiency was increased from 0.55 to 0.6 for all the droplet diameters. With increase in relative humidity the compressor characteristic shifted closer to the compressor's dry operating curve. This behavior was found to be in-line with the findings of White and Meacock [4]. The evaporation rate of the water droplets is dependent on droplet size and moisture content of the air among other factors. Thus, a larger droplet size or high RH slows down the evaporation rate and causes less energy to be absorbed from the fluid, reducing the extent of the cooling effect. These droplets tend to migrate towards the blade tip region and may influence the aerodynamics of tip leakage flow.

For improved performance of the axial flow compressor, it is desirable to operate it at lower relative humidity, preferably less than 30% and at lower droplet diameter of around 10 μm. The lower relative humidity help maintain the high pressure ratio, whereas, lower droplet diameter improves the isentropic efficiency of the axial flow compressor.

9. Conclusions

The obtained results demonstrate the effect of humid air and water ingestion on the aerodynamic performance of an axial flow compressor across its operating range. It was observed that the humid air reduces the pressure rise and the compressor efficiency by 8% and 5%, respectively, whereas water ingestion found to increase the compressor efficiency. The highest improvement in compressor efficiency was about 9% for the droplet diameter of 10 μm and relative humidity of 10%. The compressor performance characteristics was almost independent of the water droplet diameter. Hence, the water droplet diameter does not found to play a major role in the compressor performance with water ingestion. At higher flow coefficient, the water ingestion led to the increased pressure rise, whereas, at lower flow coefficient, the pressure rise decreased as compared to that of dry air.

REFERENCES

[1]. *A.B. Reid, R.S. Natalie, J.C. Fabian and N.L. Key,* "Humidity Effects on Experimental Compressor Performance — Corrected Conditions for Real Gases", Proceedings of ASME Turbo Expo: Turbine Technical Conference and Exposition, Düsseldorf, Germany, 2014.

[2]. *J. Rhee, J. Im, J. Kim and S.J. Song*, "Humidity effects on the aerodynamic performance of a transonic compressor cascade", International Journal of Heat and Mass Transfer, **vol. 140**, 2019, pp. 743–751.

[3]. *J.T. Tomita, L.P. Bontempo and J. R. Barbosa*, "An axial-flow compressor for operation with humid air and water injection", Proceedings of ASME TURBO EXPO, Power for Land, Sea, and Air, 2010.

[4]. *A.J. White and A.J. Meacock*, "An Evaluation of the Effects of Water Injection on Compressor Performance*",* ASME J. Eng. Gas Turbines Power, **vol. 126**, Oct. 2004, pp.748-754.

[5]. *T. Roos*, A prediction method for flow in axial compressors, Master's Thesis, University of Stellenbosch, 1995.

[6]. *Andrew Gill*, Four Quadrant Axial Flow Compressor Performance, PhD Thesis, Stellenbosch University, 2011.

[7]. *Richard Alan Hamman*, The Analysis and Optimization of an Axial Compressor, Master's Thesis, Stellenbosch University, 2015.

[8]. ANSYS CFX Solver Modeling Guide, 2011.

[9]. *F.R. Menter*, "Two-Equation Eddy-Viscosity Turbulence Models for Engineering Applications", AIAA Journal, **vol. 32**, 1994, pp. 1598-1605.

[10]. *O.A. Alduchov, R.E. Eskridge*, Improved Magnus Form Approximation of Saturation Vapor Pressure, Report, November 1997.

[11]. *J.A. Zak*, Drop Size Distributions of Fog for Five Locations Measured from Aircraft, NASA Contractor Report 4585, April 1994.

[12]. *J. Podzimek*, Droplet Concentration and Size Distribution in Haze and Fog, Studia Geophysica. et Geodaetica, **vol. 41**, 1997, pp. 277-296.

[13]. ANSYS CFX Solver Theory Guide, 2011.

[14]. *N.A. Cumpsty*, Compressor Aerodynamics, Longman Scientific & Technical, 1989.

[15]. *L. Yang, J. Zhou, S. Fan, Q. Zheng and H. Zhang*, "Method and numerical simulation for evaluating the effects of water film on the performance of low-speed axial compressor", Aerospace Science and Technology, **vol. 84**, 2019, pp. 306–317.